Summary Report

Department of Physical Sciences

Edge Cases of Neutrino Oscillation and Introduction to Particle Dark Matter Physics Phenomenology

Arsh Dhawan (IISER Bhopal)

Supervised by:
Dr.Rahul Srivastava
IISER Bhopal

March 2026

Acknowledgements

An automatic thanks goes to 'Dr. Rahul Srivastava', Associate Professor, IISER-Bhopal for allowing me to sit through the special course on 'Standard Model of Particle Physics' organized by him for off semester of 25-26 at IISER Bhopal and later accepting my request to mentor through the project during the winter of 2025.
Additional thanks to Ronak Mukherjee for his Project which formed the basis of my reading as well as my friends Arnav Kapoor,sktime,ESoC and Aaditya Negi,ToMP group(Dr. Nirmal Ganguli) for discussions.
Some other projects[2] and some extensive study measures led to some delays, I am thankful to Dr. Rahul for being patient.
Arsh Dhawan
Date of Completion:-(15/Mar/26)

Declaration of Integrity

The author of this document declares that he has not used AI in formulating this document, other than looking for references or fixing latex errors. No part of thing document is AI-written or AI-written-Human-Enhanced. Moreover, no data/equation/derivation has been taken without citation.

Contents

Chapter 1

Neutrino Oscillations in Matter: Resonant Edge Cases

[22]

1.1 Formalism of 3-Flavor Oscillations in Matter

The evolution of the neutrino flavor state $\left|\nu_f\right\rangle = (\nu_e, \nu_\mu, \nu_\tau)^T$ is governed by the Schrödinger-like equation:

$$i\frac{d}{dt}\left|\nu_f\right\rangle = \left[\frac{1}{2E}UM^2U^\dagger + V(x)\right]\left|\nu_f\right\rangle \tag{1.1}$$

where $M^2 = \text{diag}(0, \Delta m_{21}^2, \Delta m_{31}^2)$ and $V(x) = \text{diag}(A(x), 0, 0)$ is the matter potential with $A(x) = \sqrt{2}G_F n_e(x)$ [21, 23, 1], where U is of form, $U = O_{23}U_\delta O_{13}U_\delta^\dagger O_{12}$ in which O_{ij} the orthogonal rotation matrix in the ij-plane which depends on the mixing angle θ_{ij} and U_δ=diag(1,1,$e^{i\delta_{CP}}$, δ_{CP} being the Dirac-typ e CP-violating phase.
The project assumes knowledge of resonance which was covered in previous report submitted to Dr. Srivastava for Standard Model of Particle Physics term project.

1.2 Solar Neutrinos and the LMA-MSW Edge Case

In the Sun, electron neutrinos are produced in the core and propagate through a varying density $n_e(r)$. The survival probability P_{ee} in a 3-flavor framework would be given by

$$P_{ee} = \sum_{i=1}^{3} |\widetilde{U_{ei}}|^2 |U_{ei}|^2$$

Due to resonance in low and high energy limits, we have

$$P_{ee} = \begin{cases} 1 - \frac{1}{2}sin^2 2\theta_{12} & \text{if } E << 1MeV \\ sin^2 2\theta_{12} & \text{if } E >> 10MeV \end{cases} \tag{1.2}$$

The resonance occurs when the matter potential matches the oscillation frequency: $A\cos^2\theta_{13} = \Delta m_{21}^2 \cos 2\theta_{12}$. This leads to the adiabatic conversion of ν_e into ν_2. [11].

1.3 Atmospheric Neutrinos and Core-Passage Resonances

Atmospheric neutrinos traversing the Earth encounter large matter effects, particularly in the $\nu_\mu \to \nu_\tau$ channel for $L > 10,000$ km [20]. For neutrinos passing through the Earth's core, the resonance condition $A \approx \Delta m_{31}^2 \cos 2\theta_{13}$ can be met. This results in a massive enhancement of the oscillation probability. [20]. When $A = m_{31}^2 cos2\theta_{13}$, there is a resonance and thus $\theta_{13} = \frac{\pi}{4}$ and the mixing in the 1-3 sector is maximal. At the resonance the oscillations of the survival probability of electron neutrinos are maximal,

$$P_{ee} = 1 - S_{31}^2$$

while the other probabilities depend on the value of θ_{23}[21].

1.4 Supernova Neutrinos: The High-Density Limit

[1]

In core-collapse supernovae, the density profile follows $\rho \propto r^{-3}$. Two distinct resonances occur: the H-resonance (high density, Δm_{31}^2) and the L-resonance (low density, Δm_{21}^2) [14, 13]. The adiabaticity of these transitions determines the final flavor swap ratios observed on Earth. My previous report [13] show that the H-resonance occurs in the neutrino sector.
This leads to neutrino oscillation suppression inside the SNe's proto-neutron star. Hence,

$$\nu_{3m} = \nu_e$$

$$\nu_{2m} = \nu_\tau$$

$$\nu_{1m} = \nu_\mu$$

and

$$F_{1m}^0 = F_x^0, \qquad F_{2m}^0 = F_x^0, \qquad F_{3m}^0 = F_e^0$$

If we calculate flux of first eigenstate ν_1 at surface of the star. The probability of original state ν_e arrives at surface as it will be $P_H P_L$ since it has to flip to other matter eigenstate at both resonances, i.e. the flux would be $F_e^0 P_H P_L$, then the flux from muon neutrino would be $(1 - P_L)F_x^0$ and from tau would be $P_L(1 - P_H)F_x^0$. Hence,

$$F_1 = P_H P_L F_e^0 + (1 - P_H P_L)F_x^0.$$

and similarly;

$$F_2 = (P_H - P_H P_L)F_e^0 + (1 - P_H + P_H P_L)F_x^0$$

$$F_3 = (1 - P_H)F_e^0 + P_H F_x^0.$$

generally, we can write them as

$$F_i = a_i F_e^0 + (1 - a_i)F_x^0$$

,where

$$a_1 = P_H P_L, \qquad a_2 = P_H(1 - P_L)$$

$$a_3 = 1 - P_H$$

[1]**Note:** the later part of this section has been taken from previous report.

We know that

$$F_z = \sum_i |U_{zi}|^2 F_i$$

,where z is some flavour state and i represents mass states.
For electron neutrino, we can say,

$$F_e = F_e^0 \left[\sum_i |U_{ei}|^2 a_i + F_\chi^0 \left(1 - \sum_i |U_{ei}|^2 a_i \right) \right]$$

Hence the electron reaching earth can be written as

$$F_e = pF_e^0 + (1-p)F_x^0$$

with p as

$$\begin{aligned} p &= \sum_i |U_{ei}|^2 a_i \\ &= |U_{e1}|^2 P_H P_L + |U_{e2}|^2 (P_H - P_H P_L) + |U_{e3}|^2 (1 - P_H). \end{aligned} \tag{1.3}$$

and by conservation of flux

$$F_\mu + F_\tau = (1-p)\, F_e^0 + (1+p)\, F_\chi^0. \tag{1.4}$$

which gives us the final values of their fluxes, which will help us compute and compare the fluxes obtained in SNe neutrino detectors.[2]

[2]**Note:** we have not considered matter effects due to earth but they are easily computable since we know the fluxes at surface of the earth and are well aware of matter effects.

Chapter 2

Dark Matter

[33]

2.1 Why dark matter?

[32] There are a variety of observations that can be reasoned through existence of Dark Matter[38][1] but a very known and reasonable evidence would be rotation of spiral galaxies.
According to visible/baryonic density of galaxies, the velocity of should decrease with radii and at larger radii, it can be estimated to,

$$v(r) = \sqrt{\frac{G\int \rho \frac{4}{3}\pi r^3 dr}{r}} = \sqrt{GM/r} \tag{2.1}$$

at larger distances, but an opposite trend is seen where the velocity increases with radius and become constant with large distances.

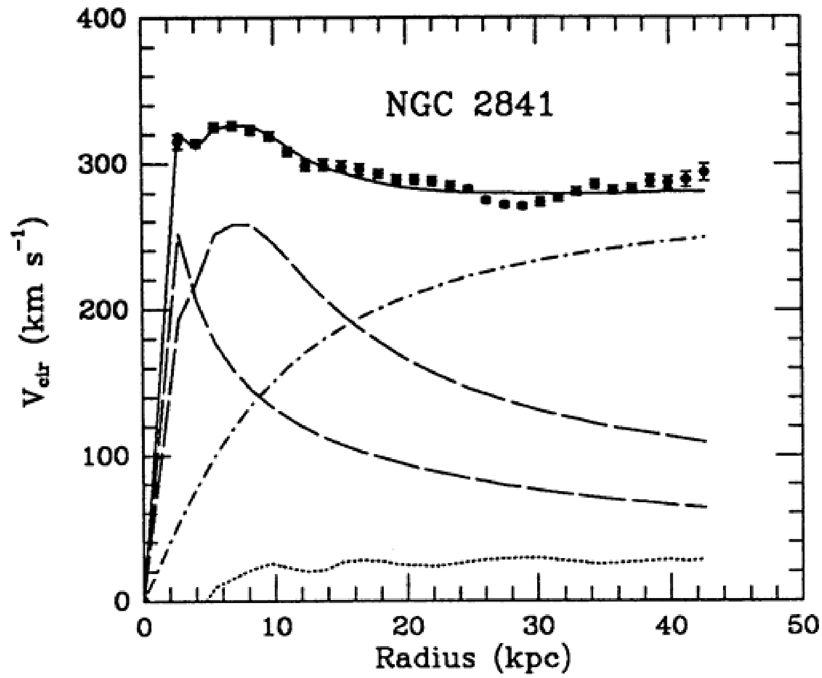

where, dashed lines are for visible components, dotted lines are for gases and dash-dotted are for dark halo. [3]

[1] One may find a few in the citation attached, though it hasn't been added to keep the nature of the report coherent.

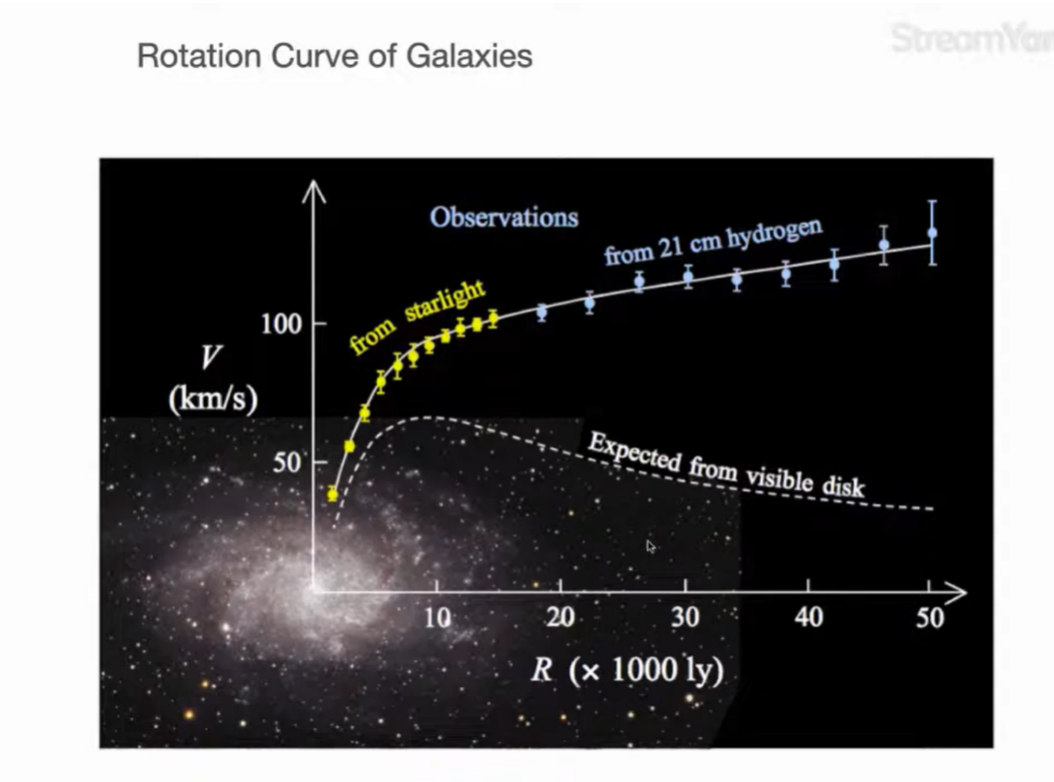

To achieve such a function, we must have a density of order r^{-2}[6]. One possible known solution is

$$\rho(r) = \frac{\rho_o}{\left(\frac{r}{R_c}\right)\left(1+\frac{r}{R_c}\right)^{3-\gamma}} \tag{2.2}$$

,which is the known density function of Milky Way,[26, 34] where R_c is scale radius and γ is inner cusp.[2]

2.2 Neutrinos as contendors for Dark Matter

[32] If a particle doesn't have charge, it has no interaction with γ. Thus, neutrinos could be a strong contendor for Dark Matter, but the problem arises from their miniscule masses.
Density of Dark Matter near the sun is estimated to be[36]

$$\rho_o = (0.3-0.4)\frac{GeV}{cm^3} \tag{2.3}$$

so to fit this density, the neutrinos should be as densely packed which is impossible as neutrinos are fermions.
Given the number density,

$$n = g_o \int \frac{d^3p}{(2\pi)^3} f(p,t) \tag{2.4}$$

or

$$n = g_o \int \frac{a^3}{(2\pi)^3} f(p,t) \tag{2.5}$$

where we have taken h=1 and $f(p,t)$ is distribution function.

$$n = \frac{g_1}{6\pi^2}\frac{4\pi}{3}p^3 = \frac{g_1}{6\pi^2}\frac{4\pi}{3}m_\nu^3 v^3 \tag{2.6}$$

[2]taking $\alpha = 1$ and $\beta = 3$.

and energy density would be

$$\rho = m_\nu n = m_\nu^4 \frac{4\pi}{6\pi^2} \frac{g_1}{3} \nu^3 \tag{2.7}$$

Now, for cosmology if neutrinos are dark matter then at cosmological limit(1000Mps)[3] in annhilations($XX \rightarrow \gamma\gamma, e^+e^-, \nu\bar{\nu}$) for relativistic limit(T>m)

$$n_{eq} = \begin{cases} g_1 \frac{1.2}{\pi^2} T^3 & \text{for boson} \\ \frac{3}{4} g_1 \frac{1.3}{\pi^2} T^2 & \text{for fermions} \end{cases} \tag{2.8}$$

and for non-relativistic limit(T<m)

$$n_{eq} = g_1 \left| \frac{mT}{2\pi} \right|^{\frac{3}{2}} e^{-\frac{m}{T}} \tag{2.9}$$

We see that at $\frac{m}{T} \rightarrow \infty$ i.e. $T \rightarrow 0$, $n_{eq} \rightarrow 0$.
i.e. if there is less p initially, they will disappear. Hence only way to survive is if they stop interacting and do not annhilate to form lighter particles.
If we take into account the scale factor a(t) in FRW Metric(when universe expands/shrinks)

$$dx' = a(t)dx$$

$$V = \frac{a^3}{a_o^3} V_o 0$$

For non interacting particles the number density,

$$n_{eq} = \frac{number}{vol} \propto a^{-3}$$

Hence,

$$\frac{d}{dt} a^3 n = 0$$

which on simplifying(simply dividing by a^3) gets us

$$\dot{n} + 3\frac{\dot{a}}{a} n = 0 \tag{2.10}$$

putting $\frac{\dot{a}}{a} = H$, we get

$$\dot{n} + 3Hn = 0 \tag{2.11}$$

A general equation in considering even the non eqm cases would be

$$\dot{n} + 3Hn = -\langle \rho v \rangle (n^2 - n_{\text{eq}}^2) \tag{2.12}$$

A general approach is highlighted in next section.

2.3 Cosmology

[4]

[3] 1 ps 3.26 Light years

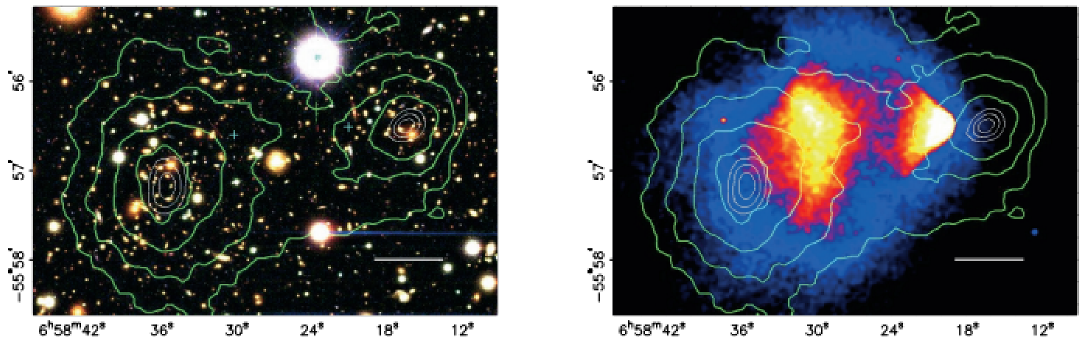

FIG. 1.—*Left panel*: Color image from the Magellan images of the merging cluster 1E 0657−558, with the white bar indicating 200 kpc at the distance of the cluster. *Right panel*: 500 ks *Chandra* image of the cluster. Shown in green contours in both panels are the weak-lensing κ reconstructions, with the outer contour levels at κ = 0.16 and increasing in steps of 0.07. The white contours show the errors on the positions of the κ peaks and correspond to 68.3%, 95.5%, and 99.7% confidence levels. The blue plus signs show the locations of the centers used to measure the masses of the plasma clouds in Table 2.

[7]

In order to create a cosmological model we obviously require the following 3 things

- **Einstein equations** which relates the geometry of the Universe with the matter and energy content.
- **Metrics** which describe the symmetries.
- **Equation of state** which describe the physical properties of the matter and energy content.

The Einstein field equation[8] can be written as

$$R_{\mu\nu} - \frac{1}{2} g_{\mu\nu} R = -\frac{8\pi G_N}{c^4} T_{\mu\nu} + \Lambda g_{\mu\nu} \tag{2.13}$$

,where $R_{\mu\nu}$ and R are, the Ricci tensor and scalar, respectively which describe the contraction of the Riemann curvature tensor.[35]

Also, $g_{\mu\nu}$is metric tensor, G_N is Newton's constant, $T_{\mu\nu}$ is energy-momentum tensor, and Λ is the cosmological constant.

The properties of isotropy and homogeneity imply a specific form of the metric which can be represented as,

$$ds^2 = -c^2 dt^2 + a(t)^2 \left(\frac{dr^2}{1 - kr^2} + r^2 d\Omega^2 \right)$$

where a(t) is the scale factor which we have used before and, the constant k describes the spatial curvature and can take the values k = -1, 0, +1.

The Einstein equations can be solved with this metric, with one of its components leading to the Friedmann equation

$$\left(\frac{\dot{a}}{a} \right)^2 + \frac{k}{a^2} = \frac{8\pi G_N}{3} \rho_{\text{tot}} \tag{2.14}$$

with $\rho_t ot$ being the total average energy density of the universe.

Introducing the hubble parameter and considering a flat universe, the energy density equals the critical density i.e.

$$\rho_c = \frac{3H^2}{8\pi G_N}$$

we also defind Ω_i with respect to some species 'i' as

$$\Omega_i = \frac{\rho_i}{\rho_c}$$

Thus,

$$\Omega = \Sigma_i \Omega_i = \Sigma_i \frac{\rho_i}{\rho_c}$$

Also, wrt Friedmann eqn,

$$\Omega - 1 = \frac{k}{H^2 a^2} \tag{2.15}$$

In future, we will also refer to Ω_M for matter and Ω_R for radiation and define $\Omega_K = \frac{-k}{a_o^2 H_o^2}$

2.4 Thermodynamics and Boltzmann Equation

[33, 15] A particle species in the early Universe has to interact sufficiently or it will fall out of local thermodynamic equilibrium. Roughly speaking, when its interaction rate drops below the expansion rate of the Universe, the equilibrium can no longer be maintained and the particle is said to be decoupled. This concept was discussed briefly in section (2.2) There are many ways to get the desired equation (2.12), we can apply various approaches from QFT to Statistical Mechanics. Let us refer to a mixed approach from GR and Statistical Mechanics.[33, 4]. We introduce Einstien Field equation given by,

$$G_{\mu\nu} = 8\pi G T_{\mu\nu}, \tag{2.16}$$

and phase space distribution function given by

$$f(x^\mu, p^\nu), \tag{2.17}$$

Thus, the Energy-momentum tensor can be written as:[32]

$$T_{\mu\nu}(x) = \int \frac{d^3p}{(2\pi)^3} \frac{p_\mu p_\nu}{p^0} f(x,p) \tag{2.18}$$

Since,

$$\nabla_\mu \left(R^{\mu\nu} - \frac{1}{2} g^{\mu\nu} R \right) = \nabla_\mu G^{\mu\nu} = 0 \quad \Rightarrow \quad \nabla_\mu T^{\mu\nu} = 0 \tag{2.19}$$

If we substitute the value of $T_{\mu\nu}$ in this equation, we will get

$$\nabla_\mu T^{\mu\nu} = \int \frac{d^3p}{(2\pi)^3} \nabla_\mu \left(\frac{p^\mu p^\nu}{p^0} f \right). \tag{2.20}$$

let's evaluate the expression inside the integral. we can expand it to,

$$\nabla_\mu \left(\frac{p^\mu p^\nu}{p^0} f \right) = \frac{p^\mu p^\nu}{p^0} \partial_\mu f + f \nabla_\mu \left(\frac{p^\mu p^\nu}{p^0} \right). \tag{2.21}$$

and since the covariant derivative of the momentum is given by

$$\nabla_\mu p^\alpha = -\Gamma^\alpha_{\mu\beta} p^\beta, \tag{2.22}$$

Hence,

$$\nabla_\mu (p^\mu p^\nu) = -\Gamma^\mu_{\mu\beta} p^\beta p^\nu - \Gamma^\nu_{\mu\beta} p^\mu p^\beta. \tag{2.23}$$

Thus,

$$\nabla_\mu T^{\mu\nu} = \int \frac{d^3p}{(2\pi)^3 p^0} p^\nu \left(p^\mu \frac{\partial f}{\partial x^\mu} - \Gamma^\alpha_{\mu\beta} p^\mu p^\beta \frac{\partial f}{\partial p^\alpha} \right) = 0 \tag{2.24}$$

We see that the formulated distribution actually satistifes relativistic Boltzmann equation.[4]

[4] It is told in Bertone, I am not familiar with it.

Thus, we can rewrite it as,

$$p^{\mu}\frac{\partial f}{\partial x^{\mu}}-\Gamma^{\alpha}_{\mu\beta}p^{\mu}p^{\beta}\frac{\partial f}{\partial p^{\alpha}}=C[f], \tag{3.6}$$

where C is collision operator, describing the interactions of the particle species considered.
Thus, the Liouville operator becomes,

$$\mathscr{L}[f]=p^{\mu}\frac{\partial f}{\partial x_{\mu}}-\Gamma^{i}_{\alpha\beta}p^{\alpha}p^{\beta}\frac{\partial f}{\partial p^{i}} \tag{2.25}$$

If we consider the geodesic equation (equation of motion for a free particle moving in curved space-time/footnotemotion under gravity alone, with no non-gravitational forces.),[5]

$$\frac{dp^{\mu}}{d\lambda}+\Gamma^{\mu}_{\alpha\beta}p^{\alpha}p^{\beta}=0 \tag{2.26}$$

This in FRW universe gives us,[6]

$$\mathscr{L}[f]=E\left(\frac{\partial f}{\partial t}-Hp\frac{\partial f}{\partial p}\right)=E\frac{\partial f}{\partial t}-Hp^{2}\frac{\partial f}{\partial E}, \tag{2.27}$$

Thus,

$$\mathscr{C}[f]=\frac{\partial f}{\partial t}-Hp\frac{\partial f}{\partial p} \tag{2.28}$$

where we have redefined,

$$\frac{\mathscr{C}[f]}{E}\equiv\mathscr{C}[f].$$

Using the equation for number density, integrating the boltzmann equation yields

$$g\int\frac{d^{3}p}{(2/pi)^{3}}\mathscr{L}[f]=\dot{n}+3Hn=g\int\frac{d^{3}p}{(2/pi)^{3}}\frac{\mathscr{C}[f]}{E} \tag{2.29}$$

which considering CPT Symmetry, equilibrium and balance condition($f_{X}^{eq}f_{\bar{X}}^{eq}=f_{a}^{eq}f_{b}^{eq}$)[7], turns

$$\begin{aligned}\int\frac{d^{3}p_{X}}{E_{X}}\mathscr{C}[f_{X}]=\int\frac{g_{X}\,d^{3}p_{X}}{(2\pi)^{3}2E_{X}}\frac{g_{\bar{X}}\,d^{3}p_{\bar{X}}}{(2\pi)^{3}2E_{\bar{X}}}\frac{g_{a}\,d^{3}p_{a}}{(2\pi)^{3}2E_{a}}\frac{g_{b}\,d^{3}p_{b}}{(2\pi)^{3}2E_{b}}\\ \times(2\pi)^{4}\delta^{(4)}(p_{X}+p_{\bar{X}}-p_{a}-p_{b})\\ \times\left[|\mathscr{M}|^{2}_{X\bar{X}\to ab}f_{X}f_{\bar{X}}-|\mathscr{M}|^{2}_{ab\to X\bar{X}}f_{a}f_{b}\right]\end{aligned} \tag{2.30}$$

into[8]

$$g\int\frac{d^{3}p}{(2\pi)^{3}E}\mathscr{C}[f]=-\langle\sigma v\rangle(n^{2}-n_{eq}^{2}) \tag{2.31}$$

where $\langle\sigma v\rangle$ is thermally averaged cross section obtained by

$$\langle\sigma v\rangle\equiv\frac{\int d^{3}p_{X}\,d^{3}p_{\bar{X}}\,\sigma v\,f_{X}^{\text{eq}}f_{\bar{X}}^{\text{eq}}}{\int d^{3}p_{X}\,d^{3}p_{\bar{X}}\,f_{X}^{\text{eq}}f_{\bar{X}}^{\text{eq}}}. \tag{2.32}$$

which will get us

$$\dot{n}+3Hn=-\langle\rho v\rangle(n^{2}-n_{\text{eq}}^{2}) \tag{2.33}$$

[5] in momentum form
[6] derivation given in Appendix A
[7] we are considering annhilations as stated before $X\bar{X}\to ab$.
[8] Notice the square bracket term in equation 2.30, CPT, eqm and balance condition turn this to $(n_{eq}^{2}-n^{2})$

as mentioned.

Chapter 3

Dark Matter Phenomenology

3.1 Freeze Out Mechanism and Relic Density Composition

[9] [4, 33] Following our previous derivation of the Liouville operator in the Friedmann-Robertson-Walker (FRW) metric, we now establish the evolution of the macroscopic number density n of the Dark Matter (DM) candidate.

By integrating the distribution function $f(\mathbf{p}, t)$ over the momentum space, we obtain the unintegrated Boltzmann equation. For a particle species χ undergoing annihilation $\chi\bar{\chi} \leftrightarrow X\bar{X}$ (where X represents Standard Model states in thermal equilibrium), the evolution of the number density n_χ is governed by:

$$\frac{dn_\chi}{dt} + 3Hn_\chi = -\langle\sigma v\rangle(n_\chi^2 - (n_\chi^{eq})^2) \tag{3.1}$$

where $H = \dot{a}/a$ is the Hubble parameter, $\langle\sigma v\rangle$ is the thermally averaged annihilation cross-section multiplied by the relative velocity, and n_χ^{eq} is the equilibrium number density.

To absorb the effects of the expansion of the universe, it is highly convenient to work with the yield

$$Y = \frac{n_\chi}{s}$$

, where s is the entropy density of the universe and

$$s = 2\pi^2 \frac{g_* T^3}{45}$$

and g_* counts number of relativistic degrees of freedom. Since the expansion is adiabatic, $sa^3 =$ constant, giving [29]

$$\dot{n} + 3Hn = s\dot{Y} \tag{3.2}$$

Thus,

$$s\dot{Y} = -\langle\rho v\rangle s^2(Y^2 - Y_{\text{eq}}^2) \tag{3.3}$$

Remember, in non relativistic limit

$$n^{\text{eq}} = g\left(\frac{mT}{2\pi}\right)^{3/2} e^{-m/T}, \tag{3.4}$$

thus, we get,

$$\frac{dY}{dx} = -\frac{\langle\rho v\rangle s}{Hx}(Y^2 - Y_{eq}^2) \tag{3.5}$$

The cross section on expanding in powers of v^2 get us an approximation

$$\langle \rho v \rangle = a + \frac{b}{x} \tag{3.6}$$

taking $\Delta = Y - Y_{eq}$ we get

$$\Delta' = -Y'_{\text{eq}} - f(x)\Delta(2Y_{\text{eq}} + \Delta), \tag{3.7}$$

with

$$f(x) = \sqrt{\frac{\pi g_*}{45}}\, m M_{\text{Pl}} \left(a + \frac{6b}{x}\right) x^{-2}. \tag{3.8}$$

$$\frac{dY}{dx} = -\sqrt{\frac{\pi g_*(T)}{45}} \frac{M_{pl} m_\chi}{x^2} \langle \sigma v \rangle (Y^2 - Y_{eq}^2) \tag{3.9}$$

where $M_{pl} \approx 1.22 \times 10^{19}$ GeV is the Planck mass, and $g_*(T)$ represents the effective number of relativistic degrees of freedom.

3.1.1 Freeze Out and Relic Density

At high temperatures ($x \ll 1$), DM is in thermal equilibrium, and $Y \approx Y_{eq}$. As the temperature drops below the DM mass ($x \gtrsim 1$), Y_{eq} becomes Boltzmann suppressed: $Y_{eq} \propto x^{3/2} e^{-x}$. Eventually, the interaction rate $\Gamma = n_\chi \langle \sigma v \rangle$ drops below the Hubble expansion rate $H(T)$, leading to chemical decoupling or "freeze-out". The freeze-out temperature x_f is determined iteratively by the condition $\Delta(x_f) = cY_{eq}(x_f)$ with $c \approx \mathcal{O}(1)$, yielding:

$$x_f = \ln\left(c(c+2)\sqrt{\frac{45}{8\pi^4}} \frac{g}{g_*^{1/2}} M_{Pl} m_\chi \frac{\langle \sigma v \rangle}{x_f^{1/2}} \right) \tag{3.10}$$

For a typical Weakly Interacting Massive Particle (WIMP) with $m_\chi \sim 100$ GeV and weak-scale cross-sections, $x_f \approx 20 \sim 25$.

Integrating the Boltzmann equation from x_f to today ($x_0 \to \infty$) yields the asymptotic yield Y_∞.

$$Y_\infty = \int_{x_F}^{\infty} f(x)\, dx$$

Thus,

$$Y_\infty \simeq \sqrt{\frac{\pi g_*}{45}} \frac{M_{\text{pl}} m}{x_F} \left(a + \frac{3b}{x_F}\right). \tag{3.11}$$

The present-day relic density can be found by$\rho_x = m_x n_x$ which becomes $m_x s_o Y_\infty$. The relic abundance is then expressed as:

$$\Omega_x h^2 = \frac{\rho_x}{\rho_c / h^2} \tag{3.12}$$

Since, $\rho_c / h^2 = (1.05)10^{-5} GeV cm^{-3}$

$$\Omega_\chi h^2 = 1.07 \times 10^9\, \text{GeV}^{-1} \frac{x_F}{M_{\text{Pl}} \sqrt{g_*}} \frac{1}{a + 3b/x_F}, \tag{3.13}$$

which can be approximated to

$$\Omega_X h^2 \approx \frac{m_\chi s_0 Y_\infty}{\rho_c / h^2} \approx \frac{3 \times 10^{-27}\ \text{cm}^3\ \text{s}^{-1}}{\langle \sigma v \rangle} \tag{3.14}$$

This remarkable result, where the relic density depends almost exclusively on the annihilation cross-section, is known as the "WIMP Miracle". A cross-section of $\langle \sigma v \rangle \approx 3 \times 10^{-26}$ cm^3 s^{-1} naturally reproduces the observed Planck collaboration value $\Omega_{DM} h^2 \approx 0.12$ [4].

3.2 Contendors for Dark Matter

3.2.1 Neutrinos(SM)

As discussed before, the problem with SM neutrinos being contendors for DM lies in their miniscule mass which puts their relic density to;

$$\Omega_\nu h^2 = \Sigma_{i=1}^3 \frac{m_i}{93eV} \tag{3.15}$$

From constraints on neutrino masses from tritium β-decay experiments at Troitsk and Mainz [39], we get $m_\nu < 2.05eV$ which implies an upper bound on the total neutrino relic density of

$$\Omega_\nu h^2 < 0.07 \tag{3.16}$$

Thus SM neutrinos can not be major components of DM.

3.2.2 Sterile Neutrinos

First proposed by Dodelson and Widrow[16] in '97, there has been significant work on the topic primarily by Prof. Srubabati Goswami[12, 10].Sterile neutrinos are right-handed SM singlets introduced to generate active neutrino masses via the seesaw mechanism.
A keV-scale sterile neutrino can serve as Warm Dark Matter (WDM). They are produced in the early universe via active-sterile mixing (the Dodelson-Widrow mechanism) or resonant production with a primordial lepton asymmetry (Shi-Fuller mechanism). Their defining phenomenological signature is a two-body radiative decay $\nu_s \to \nu_a + \gamma$, resulting in a monochromatic X-ray line at $E_\gamma = m_s/2$, which has motivated extensive searches in galaxy clusters using space telescopes like Chandra and XMM-Newton.

3.2.3 Axions

The QCD axion arises organically from the Peccei-Quinn (PQ) solution to the strong CP problem. The QCD Lagrangian contains a CP-violating term $\frac{\theta}{32\pi^2} G_{\mu\nu}\tilde{G}^{\mu\nu}$, which induces a non-zero neutron electric dipole moment (nEDM). Experimental bounds limit $|\theta| \lesssim 10^{-10}$. Peccei and Quinn postulated a global $U(1)_{PQ}$ symmetry, spontaneously broken at a scale f_a, promoting θ to a dynamical field: the axion a. The axion acquires a small mass via instanton effects at the QCD phase transition:

$$m_a \simeq 5.7\ \mu\text{eV}\left(\frac{10^{12}\ \text{GeV}}{f_a}\right) \tag{3.17}$$

Axions are produced non-thermally via the vacuum misalignment mechanism and are an excellent cold dark matter (CDM) candidate, currently hunted by microwave cavity haloscopes like ADMX. Laboratory searches, stellar cooling and the dynamics of supernova 1987A constrain axions to be very light $<\approx 0.01eV$
. They are expected to be extremely weakly interacting with ordinary particles, which implies that they were not in thermal equilibrium in the early universe.
We do not compute the relic denisty for axions as it relies too much on assumptions made and there is lack of real data.

3.2.4 WiMP

[30] WIMPs (Weakly Interacting Massive Particles) are stable particles left over from Big Bang and has weak interactions. Their mass is in range of 2GeV to about 100 TeV.
Theory states if present in halo, it can be found directly in low-background laboratory detectors, or indirectly

by observing energetic neutrinos from WIMPs that have accumulated and annihilated in the Sun and/or Earth.
It is said to have a greater interaction cross section than axions, axinos, gravitinos, and sterile neutrinos, making them an appealing experimental target. Their huge masses and weak-scale annihilation cross section naturally produces the observed relic abundance through thermal freeze-out

$$\Omega_{WiMP}h^2 \approx \frac{3(10)^{-27}cm^3/s}{\langle \sigma v \rangle} \tag{3.18}$$

WIMPs are being searched for through:

- direct detection(nuclear recoil)
- indirect detection(annhilation signals)
- collider searches

The search is still going on. It's still one of the most researched candidates.

3.2.5 Primordial Black Holes

Known as a contendor to Dark Matter since the inception of Hawking radiation [24]. They are cold, non-baryonic and stable, and can be formed in the right abundance to be the DM. Zel'dovich and Novikov (1967) and Hawking (1971) found that Primordial Black Holes may form from overdensities in the early Universe. Later it was found that phase transitions, or topological defects could also produce it. They can have variety of mass upto many solar masses and starting from mere asteroids.
We may constraint it using

- Hawking radiation/evaporation
- CMB data
- Gravitational Wave (Observatories like LiGO)

3.2.6 Supersymmetric Dark Matter

A few of the known candidates could be;

- Neutralinos
- Sneutrinos
- Gravitinos
  superpartners of the graviton in supersymmetric models
- Axinos
  superpartners of Axions. Can exist as either cold or hot or warm Dark Matter.

Chapter 4

Detection

4.1 Direct Detection

[38]

4.1.1 Working Principle

Since, Earth resides within a DM halo and moves through it with a velocity $v \sim 220$ km/s. Direct detection aims to observe the elastic scattering of DM[1] off target nuclei in ultra-sensitive laboratory detectors. The expected energy of the recoiling nucleus varies with DM partocle and is generally in the range $\sim 1-100$ keV for WiMPs. The event rate relies heavily on the local DM density ($\rho_0 \approx 0.3$ GeV/cm^3) and the DM velocity distribution $f(\mathbf{v})$ in the galactic rest frame.

4.1.2 Direct Detection Experiment Setup

The current leaders in the direct detection field are dual-phase (liquid/gas) noble element Time Projection Chambers (TPCs), predominantly utilizing Xenon (e.g., XENONnT, LZ, PandaX-4T) or Argon (DarkSide).

When a WIMP scatters off a Xenon nucleus, the deposited energy produces two observable signals: 1. **S1 (Scintillation):** Prompt UV photons ($\sim$ 175 nm) detected by Photomultiplier Tubes (PMTs) at the top and bottom of the chamber. 2. **S2 (Ionization):** Electrons freed by the recoil drift upwards under an applied electric field into the gaseous phase, where a stronger field extracts them, creating proportional scintillation (S2).

The 3D position of the event is reconstructed from the hit pattern of the S2 signal on the top PMT array (X-Y) and the time delay between S1 and S2 (Z, or depth). The ratio $S2/S1$ is the primary discriminator: Nuclear Recoils (NR) from WIMPs or neutrons produce heavily ionizing tracks with a lower $S2/S1$ ratio compared to Electron Recoils (ER) from β/γ radioactive backgrounds. To achieve the ultra-low background environment, these detectors are placed deep underground (e.g., LNGS in Italy, SURF in USA) to shield against cosmic ray muons, and are submerged in active water Cherenkov or gadolinium-doped vetoes.

4.1.3 Computing Direct Detection Nucleus Scattering

Since the experiments use heavy nuclei ($A \sim 131$ for Xenon). For Spin-Independent scattering, the WIMP scatters coherently off the entire nucleus, yielding an A^2 enhancement in the cross-section. The differential

[1] Personal Note: Remember Super-KamioKande

event rate (events per unit mass, per unit energy, per unit time) is given by:

$$\frac{dR}{dE_R} = \frac{\rho_0}{m_N m_\chi} \int_{v_{min}}^{\infty} v f(\mathbf{v}) dv \frac{d\sigma_{WN}}{dE_R} \tag{4.1}$$

where $v_{min} = \sqrt{m_N E_R / (2\mu_{WN}^2)}$ is the minimum WIMP velocity required to produce a recoil energy E_R. The differential cross-section for the nucleus N is expressed as:

$$\frac{d\sigma_{WN}}{dE_R} = \frac{m_N}{2\mu_{WN}^2 v^2} \sigma_0 F^2(E_R) \tag{4.2}$$

where σ_0 is the zero-momentum transfer cross-section ($\sigma_0 \propto A^2 \sigma_p$), and $F(E_R)$ is the nuclear form factor, which accounts for the loss of coherence at high momentum transfer $q = \sqrt{2m_N E_R}$. $F(q)$ is simply the Fourier transform of the nucleon density distribution.
The **Spin Independent(SI)** scattering generally scales with A^2 while the **Spin Dependent(SD)**scattering is sensitive to the Nuclear Spin content.

4.1.4 Indirect Detection

Indirect detection seeks the annihilation or decay products of DM from regions of high DM density (e.g., the Galactic Center, dwarf spheroidal galaxies). The primary signals include:

- **Gamma rays:** From continuous fragmentation (e.g., $\chi\chi \to b\bar{b} \to \gamma\gamma$) or monochromatic line signals ($\chi\chi \to \gamma\gamma$). The expected flux is

$$\frac{d\Phi}{dE} = \frac{\langle \sigma v \rangle}{8\pi m_\chi^2} \sum_f B_f \frac{dN_f}{dE} \int_{\text{l.o.s.}} \rho^2(r)\, dl \tag{4.3}$$

- **Antimatter:** Positrons (e^+) and antiprotons ($\bar{p}$) detected by AMS-02.

- **Neutrinos:** High-energy neutrinos from DM annihilation in the core of the Sun or Earth, sought by IceCube.

4.2 Scalar WIMP Scattering via Higgs Exchange in MSSM

[2] [4, 27] Taking DM as scalar which interact with nucleus via Higgs.
We derive the spin-independent elastic scattering cross section for a neutralino WIMP, isolating the contribution from Higgs exchange. All steps follow the effective-operator approach.

[2] Minimal Supersymmetric Standard Model

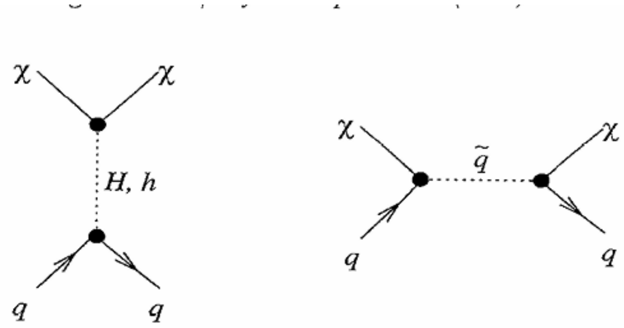

Fig. 20. Feynman diagrams contributing to the scalar elastic-scattering amplitude of a neutralino from quarks.

4.2.1 Effective Lagrangian and Higgs Contribution to a_q

The low-energy scalar interaction is

$$\mathscr{L}_{\text{scalar}} = a_q \bar{\chi}\chi\, \bar{q}q. \tag{4.4}$$

where a_q is WIMP-quark coupling. The Higgs-exchange part of a_q (t-channel h, H exchange) is

$$a_q = -\frac{1}{2(m_{1i}^2 - m_\chi^2)}\mathrm{Re}\Big[(X_i)(Y_i)^*\Big] - \frac{1}{2(m_{2i}^2 - m_\chi^2)}\mathrm{Re}\Big[(W_i)(V_i)^*\Big] \quad -\frac{g m_q}{4 m_W B}\Big[\mathrm{Re}\big(\delta_1[gN_{12} - g' N_{11}]\big)\, DC\left(-\frac{1}{m_H^2} + \frac{1}{m_h^2}\right) \quad + \mathrm{Re}\big(\delta_2[gN_{12} - g' N_{11}]\big)\left(\frac{D^2}{m_H^2} + \frac{C^2}{m_h^2}\right)\Big] \tag{4.5}$$

where

$$X_i \equiv \eta_{11}^* \frac{g m_q N_{1,5-i}^*}{2 m_W B} - \eta_{12}^* e_i g' N_{11}^*, \tag{4.6}$$

$$Y_i \equiv \eta_{11}^* \left(\frac{y_i}{2} g' N_{11} + g T_{3i} N_{12}\right) + \eta_{12}^* \frac{g m_q N_{1,5-i}}{2 m_W B}, \tag{4.7}$$

$$W_i \equiv \eta_{21}^* \frac{g m_q N_{1,5-i}^*}{2 m_W B} - \eta_{22}^* e_i g' N_{11}^*, \tag{4.8}$$

$$V_i \equiv \eta_{22}^* \frac{g m_q N_{1,5-i}^*}{2 m_W B} + \eta_{21}^* \left(\frac{y_i}{2} g' N_{11} + g T_{3i} N_{12}\right) \tag{4.9}$$

where y_i and T_{3i} denote hypercharge and isospin, and

$$\begin{aligned} \delta_1 &= N_{13}(N_{14}), & \delta_2 &= N_{14}(-N_{13}), \\ B &= \sin\beta\,(\cos\beta), & C &= \sin\alpha\,(\cos\alpha), \\ D &= \cos\alpha\,(-\sin\alpha). \end{aligned} \tag{4.10}$$

4.2.2 WIMP–Nucleon Coupling

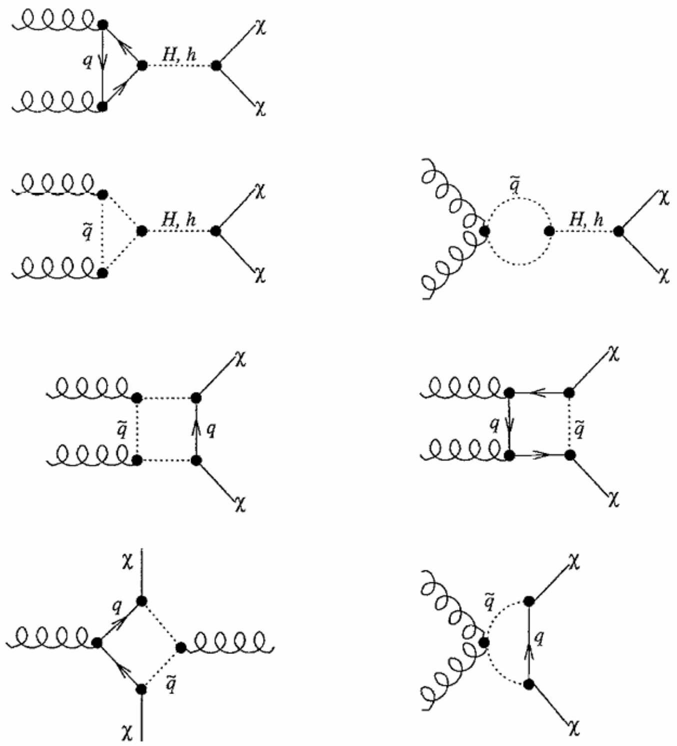

Fig. 21. Feynman diagrams contributing to the gluonic interaction with neutralinos, which contributes to the scalar elastic-scattering amplitude for neutralinos from nuclei.

[28]

The nucleon-level coupling is obtained from the matrix elements $\langle N|\bar{q}q|N\rangle$:

$$f_{p,n} = \sum_{q=u,d,s} f_{Tq}^{(p,n)}\, a_q \frac{m_{p,n}}{m_q} + \frac{2}{27} f_{TG}^{(p,n)} \sum_{q=c,b,t} a_q \frac{m_{p,n}}{m_q}, \tag{4.11}$$

with $f_{TG}^{(p,n)} = 1 - \sum_{q=u,d,s} f_{Tq}^{(p,n)}$ and $f_{Tu}^{(p)} = 0.020 \pm 0.004$, $f_{Td}^{(p)} = 0.026 \pm 0.005$, $f_{Ts}^{(p)} = 0.118 \pm 0.062$, $f_{Tu}^{(n)} = 0.014 \pm 0.003$, $f_{Td}^{(n)} = 0.036 \pm 0.008$ and $f_{Ts}^{(n)} = 0.118 \pm 0.062$.

4.2.3 Zero-Momentum-Transfer Cross Section

In the non-relativistic limit the amplitude is $\mathcal{M} \approx 4 m_\chi m_N f_{p,n}$. The total cross section is

$$\sigma_{\text{scalar}} = \frac{4\mu^2}{\pi} f_{p,n}^2, \tag{4.12}$$

where $\mu = m_\chi m_N/(m_\chi + m_N)$ is the reduced mass ($\mu \simeq m_{p,n}$ for $m_\chi \gtrsim 10\,\text{GeV}$).

For the nucleus (Z protons, $A - Z$ neutrons):

$$\sigma = \frac{4\mu^2}{\pi}\big(Z f_p + (A-Z) f_n\big)^2. \tag{4.13}$$

4.2.4 Finite-Momentum Form Factor

The differential cross section acquires the nuclear form factor (Woods-Saxon)[19]:

$$F(Q) = \left(\frac{3 j_1(qR_1)}{qR_1}\right)^2 \exp\left[-(qs)^2\right], \qquad q = \sqrt{2 m_N Q}. \tag{4.14}$$

where $j1$ is the first spherical bessel function and the momentum transferred is $q = \sqrt{smNQ}$. R_1 is given by $\sqrt{R^2 - 5s^2}$, where R and s are approximately equal to 1.2fm$A^{1/3}$ and 1fm, respectively.
It can also be written in a simpler form, though not so accurate,

$$F(Q) = exp[-Q/2Q_0] \tag{4.15}$$

Here, Q is the energy tranferred from the WIMP to the target and $Q_0 = 1.5/(m_N R_0^2)$ where $R0 = 10^{-13} cm[0.3 + 0.91(m_N/GeV)^{1/3}]$.

This completes the derivation from the MSSM Lagrangian to the observable nuclear cross section via Higgs exchange.
For detailed calculation refer to Appendix B.

Bibliography

[1] Evgeny K Akhmedov et al. "Series expansions for three-flavor neutrino oscillation probabilities in matter". In: *Journal of High Energy Physics* 2004.04 (May 2004), pp. 078–078. ISSN: 1029-8479. DOI: 10.1088/1126-6708/2004/04/078. URL: http://dx.doi.org/10.1088/1126-6708/2004/04/078.

[2] Georgios Ampatzidis. "The Unsuccessful Self-treatment of a Case of 'Writer's Block': A Replication in Science Education". In: *Journal of Trial and Error* (Jan. 2022).

[3] K. G. Begeman, A. H. Broeils, and R. H. Sanders. "Extended rotation curves of spiral galaxies: dark haloes and modified dynamics". In: *Monthly Notices of the Royal Astronomical Society* 249.3 (Apr. 1991), pp. 523–537. ISSN: 0035-8711. DOI: 10.1093/mnras/249.3.523. eprint: https://academic.oup.com/mnras/article-pdf/249/3/523/18160929/mnras249-0523.pdf. URL: https://doi.org/10.1093/mnras/249.3.523.

[4] Gianfranco Bertone, Dan Hooper, and Joseph Silk. "Particle Dark Matter: Evidence, Candidates and Constraints". In: *Physics Reports* 405 (2005).

[5] Anthony Challinor. *Advanced Cosmology: Background FRW universe and thermal history*. Lecture notes, available online. Part of the "Early Universe" course. URL: https://cosmologist.info/teaching/EU/notes_eu1.pdf. n.d. URL: https://cosmologist.info/teaching/EU/notes_eu1.pdf.

[6] Marco Cirelli et al. "PPPC 4 DM ID: a poor particle physicist cookbook for dark matter indirect detection". In: *Journal of Cosmology and Astroparticle Physics* 2011.3, 051 (Mar. 2011), p. 051. DOI: 10.1088/1475-7516/2011/03/051. arXiv: 1012.4515 [hep-ph].

[7] Douglas Clowe et al. "A Direct Empirical Proof of the Existence of Dark Matter". In: *The Astrophysical Journal* 648.2 (Aug. 2006), pp. L109–L113. ISSN: 1538-4357. DOI: 10.1086/508162. URL: http://dx.doi.org/10.1086/508162.

[8] R. d'Inverno. *Introducing Einstein's relativity*. 1992. ISBN: 978-0-19-859686-8.

[9] *Dark Matter Lectures*. https://youtube.com/playlist?list=PLu8WcRGLwtfbeJzdNE5t86svDQ8-jXDdZ. YouTube playlist. n.d. (Visited on 04/17/2026).

[10] Arindam Das et al. "Freeze-in production of sterile neutrino dark matter in a gauged U(1) model with inverse seesaw". In: *Nuclear Physics B* 1004, 116568 (July 2024), p. 116568. DOI: 10.1016/j.nuclphysb.2024.116568. arXiv: 2104.13986 [hep-ph].

[11] Peter B. Denton and Charles Gourley. "Determining the Density of the Sun with Neutrinos". In: *arXiv:2502.17546v2* (2025).

[12] P. S. Bhupal Dev et al. *Opening up New Parameter Space for Sterile Neutrino Dark Matter*. 2025. arXiv: 2505.22463 [hep-ph]. URL: https://arxiv.org/abs/2505.22463.

[13] Arsh Dhawan. "Supernovae Neutrino Oscillations". In: (2025).

[14] Amol S. Dighe and Alexei Yu. Smirnov. "Identifying the neutrino mass spectrum from the neutrino bsantos2023effectsquantumdecoherencefutureurst from a supernova". In: *Phys. Rev. D* 62 (2000).

[15] Scott Dodelson. *Modern Cosmology*. Amsterdam: Academic Press, 2003. ISBN: 978-0-12-219141-1.

[16] Scott Dodelson and Lawrence M. Widrow. “Sterile neutrinos as dark matter”. In: *Physical Review Letters* 72.1 (Jan. 1994), pp. 17–20. ISSN: 0031-9007. DOI: 10.1103/physrevlett.72.17. URL: http://dx.doi.org/10.1103/PhysRevLett.72.17.

[17] Manuel Drees and Mihoko M. Nojiri. “Neutralino-nucleon scattering reexamined”. In: *Physical Review D* 48.8 (1993), pp. 3483–3501. DOI: 10.1103/PhysRevD.48.3483. arXiv: hep-ph/9307208.

[18] John Ellis, Andrew Ferstl, and Keith A. Olive. “Re-evaluation of the elastic scattering of supersymmetric dark matter”. In: *Physics Letters B* 481.2-4 (2000), pp. 304–314. DOI: 10.1016/S0370-2693(00)00459-7. arXiv: hep-ph/0001005.

[19] J. Engel. “Nuclear form factors for the scattering of weakly interacting massive particles”. In: *Physics Letters B* 264.1-2 (July 1991), pp. 114–119. DOI: 10.1016/0370-2693(91)90712-Y.

[20] Raj Gandhi et al. “Large Matter Effects in $\nu_\mu \to \nu_\tau$ Oscillations”. In: *arXiv:hep-ph/0408361v3* (2004).

[21] C. Giunti, C. W. Kim, and M. Monteno. “Atmospheric neutrino oscillations with three neutrinos and a mass hierarchy”. In: *arXiv:hep-ph/9709439v2* (1998).

[22] Carlo Giunti and Chung W. Kim. *Fundamentals of Neutrino Physics and Astrophysics*. 2007. ISBN: 978-0-19-850871-7. DOI: 10.1093/acprof:oso/9780198508717.001.0001.

[23] Srubabati Goswami and Alexei Yu. Smirnov. “Solar neutrinos and 1-3 leptonic mixing”. In: *arXiv:hep-ph/0411359v4* (2005).

[24] Anne M. Green. *Primordial Black Holes as a dark matter candidate – a brief overview*. 2024. arXiv: 2402.15211 [astro-ph.CO]. URL: https://arxiv.org/abs/2402.15211.

[25] R. H. Helm. “Inelastic and Elastic Scattering of 187-Mev Electrons from Selected Even-Even Nuclei”. In: *Physical Review* 104.5 (1956), pp. 1466–1475. DOI: 10.1103/PhysRev.104.1466.

[26] Dan Hooper. “The density of dark matter in the Galactic bulge and implications for indirect detection”. In: *Physics of the Dark Universe* 15 (2017), pp. 53–56. ISSN: 2212-6864. DOI: https://doi.org/10.1016/j.dark.2016.11.005. URL: https://www.sciencedirect.com/science/article/pii/S221268641630070X.

[27] Gerard Jungman, Marc Kamionkowski, and Kim Griest. “Supersymmetric dark matter”. In: *Phys. Rept.* 267 (1996), pp. 195–373. DOI: 10.1016/0370-1573(95)00058-5. arXiv: hep-ph/9506380.

[28] Gerard Jungman, Marc Kamionkowski, and Kim Griest. “Supersymmetric dark matter”. In: *Physics Reports* 267.5-6 (1996), pp. 195–373. DOI: 10.1016/0370-1573(95)00058-5. arXiv: hep-ph/9506380.

[29] Edward W. Kolb and Michael S. Turner. *The Early Universe*. Vol. 69. Taylor and Francis, May 2019. ISBN: 978-0-429-49286-0, 978-0-201-62674-2. DOI: 10.1201/9780429492860.

[30] H. R. Krishnapriya, Arun Kenath, and Dewank Rathi. “WIMPs as Dark Matter Candidate and the Constraints on Its Mass and Cross Section Using Direct Detection Method”. In: *Preprints* (Apr. 2025). Preprint, version v1, not peer-reviewed. DOI: 10.20944/preprints202504.0499.v1. URL: https://doi.org/10.20944/preprints202504.0499.v1.

[31] J. D. Lewin and P. F. Smith. “Review of mathematics, numerical factors, and corrections for dark matter experiments based on elastic nuclear recoil”. In: *Astroparticle Physics* 6.1 (1996), pp. 87–112. DOI: 10.1016/S0927-6505(96)00047-3.

[32] S. Mohanty. *Nine Lectures on Early Universe*. https://www.youtube.com/playlist?list=PLfeQejpdUFAElca1DJbbelpXbalBEuyOy. 2016.

[33] Rounak Mukherjee. “An Overview on Dark Matter”. In: (2025).

[34] Julio F. Navarro, Carlos S. Frenk, and Simon D. M. White. “A Universal Density Profile from Hierarchical Clustering”. In: *The Astrophysical Journal* 490.2 (Dec. 1997), pp. 493–508. DOI: 10.1086/304888. arXiv: astro-ph/9611107 [astro-ph].

[35] Physics Latam. *Riemannian and Complex Geometry (RCG)*. https://www.physicslatam.com/rcg. Accessed: 2026-04-17. 2025-26.

[36] P.F. de Salas et al. “On the estimation of the local dark matter density using the rotation curve of the Milky Way”. In: *Journal of Cosmology and Astroparticle Physics* 2019.10 (Oct. 2019), pp. 037–037. ISSN: 1475-7516. DOI: 10.1088/1475-7516/2019/10/037. URL: http://dx.doi.org/10.1088/1475-7516/2019/10/037.

[37] M. A. Shifman, A. I. Vainshtein, and V. I. Zakharov. “Remarks on Higgs-boson interactions with nucleons”. In: *Physics Letters B* 78.4 (1978), pp. 443–446. DOI: 10.1016/0370-2693(78)90481-1.

[38] J. Silk et al. *Particle Dark Matter: Observations, Models and Searches*. Ed. by Gianfranco Bertone. Cambridge: Cambridge Univ. Press, 2010. ISBN: 978-1-107-65392-4. DOI: 10.1017/CBO9780511770739.

[39] Christian Weinheimer. *The neutrino mass direct measurements*. 2003. arXiv: hep-ex/0306057 [hep-ex]. URL: https://arxiv.org/abs/hep-ex/0306057.

Appendix A

[5] The general Liouville operator is the directional derivative of the distribution function f along the geodesic flow in phase space:

$$\mathscr{L}[f] \equiv p^{\mu}\frac{\partial f}{\partial x_{\mu}} - \Gamma^{i}_{\alpha\beta}p^{\alpha}p^{\beta}\frac{\partial f}{\partial p^{i}}. \tag{4.16}$$

This follows directly from the geodesic equation

$$\frac{dp^{\mu}}{d\lambda} + \Gamma^{\mu}_{\alpha\beta}p^{\alpha}p^{\beta} = 0. \tag{4.17}$$

(The second term in the first equation accounts for the momentum evolution, with the sum over the independent spatial momentum components p^i, $i = 1,2,3$.

In a flat FRW universe the metric is

$$ds^2 = -dt^2 + a(t)^2\delta_{ij}\,dx^i dx^j, \tag{4.18}$$

with Hubble parameter $H = \dot{a}/a$. The only relevant non-vanishing Christoffel symbols for the spatial components are

$$\Gamma^{i}_{0j} = H\delta^{i}_{j}. \tag{4.19}$$

Thus the geodesic equation for the spatial momenta becomes

$$\frac{dp^{i}}{d\lambda} = -\Gamma^{i}_{\alpha\beta}p^{\alpha}p^{\beta} = -2HEp^{i}, \tag{4.20}$$

where $E \equiv p^0$.

Because the universe is homogeneous and isotropic, f has no spatial dependence, so the convective term simplifies to

$$p^{\mu}\frac{\partial f}{\partial x_{\mu}} = E\frac{\partial f}{\partial t}\Big|_{p^i}. \tag{4.21}$$

(The partial with respect to t is taken at **fixed** contravariant momenta p^i.)

The momentum term is therefore

$$-\Gamma^{i}_{\alpha\beta}p^{\alpha}p^{\beta}\frac{\partial f}{\partial p^{i}} = \frac{dp^{i}}{d\lambda}\frac{\partial f}{\partial p^{i}} = -2HE\Big(p^{i}\frac{\partial f}{\partial p^{i}}\Big). \tag{4.22}$$

Let $q = \sqrt{\delta_{ij}p^i p^j}$ be the magnitude of the momentum vector. Isotropy implies $f = f(t,q)$, and the Euler operator gives

$$p^{i}\frac{\partial f}{\partial p^{i}} = q\frac{df}{dq}. \tag{4.23}$$

Hence the term becomes

$$-2HEq\frac{df}{dq}. \tag{4.24}$$

Also since,

$$E = \sqrt{m^2 + p^2} = \sqrt{m^2 + a^2 q^2}. \tag{4.25}$$

At fixed t and thus a,

$$\frac{dE}{dq}\Big|_t = \frac{a^2 q}{E} \implies \frac{df}{dq} = \frac{\partial f}{\partial E}\Big|_t \cdot \frac{a^2 q}{E}. \tag{4.26}$$

which yields

$$-2HEq \cdot \frac{a^2 q}{E}\frac{\partial f}{\partial E}\Big|_t = -2H(a^2 q^2)\frac{\partial f}{\partial E}\Big|_t = -2Hp^2\frac{\partial f}{\partial E}\Big|_t. \tag{4.27}$$

and thus,

$$\frac{\partial E}{\partial t}\Big|_q = H\frac{p^2}{E}. \tag{4.28}$$

and

$$\frac{\partial f}{\partial t}\Big|_{p^i \text{ (i.e., fixed } q)} = \frac{\partial f}{\partial t}\Big|_E + \left(H\frac{p^2}{E}\right)\frac{\partial f}{\partial E}\Big|_t. \tag{4.29}$$

Multiplying by E,

$$E\frac{\partial f}{\partial t}\Big|_q = E\frac{\partial f}{\partial t}\Big|_E + Hp^2\frac{\partial f}{\partial E}\Big|_t. \tag{4.30}$$

Adding the convective and drag contributions,

$$\begin{aligned}\mathscr{L}[f] &= \left[E\frac{\partial f}{\partial t}\Big|_E + Hp^2\frac{\partial f}{\partial E}\right] + \left[-2Hp^2\frac{\partial f}{\partial E}\right] \\ &= E\frac{\partial f}{\partial t}\Big|_E - Hp^2\frac{\partial f}{\partial E}\Big|_t.\end{aligned} \tag{4.31}$$

To obtain the equivalent second form, note that along a geodesic the physical momentum redshifts as

$$\frac{dp}{dt} = -Hp \tag{4.32}$$

(independent of mass). Because $d\lambda = dt/E$, the full derivative along the flow is

$$\frac{df}{d\lambda} = E\left(\frac{\partial f}{\partial t}\Big|_p - Hp\frac{\partial f}{\partial p}\Big|_t\right). \tag{4.33}$$

At fixed t, p and E are related by $dE/dp = p/E$, so

$$\frac{\partial f}{\partial p}\Big|_t = \frac{p}{E}\frac{\partial f}{\partial E}\Big|_t. \tag{4.34}$$

and thus we get,

$$E\left(\frac{\partial f}{\partial t} - Hp\frac{\partial f}{\partial p}\right) = E\frac{\partial f}{\partial t} - Hp^2\frac{\partial f}{\partial E}, \tag{4.35}$$

Appendix B: Detailed Derivations for Scalar WIMP Scattering via Higgs Exchange in MSSM

In this appendix, we provide the step-by-step derivation of the spin-independent elastic scattering cross section of a neutralino WIMP (χ) with a target nucleus. We focus specifically on the t-channel exchange of the CP-even Higgs bosons (h^0, H^0) within the Minimal Supersymmetric Standard Model (MSSM), which dominates the scalar interaction in the non-relativistic limit.

B.1 Effective Lagrangian and Higgs Contribution to a_q [28, 17]

At energy scales relevant to direct detection experiments (momentum transfer $\mathcal{O}(10\text{ MeV})$), the heavy Higgs bosons and squarks can be integrated out, yielding an effective four-fermion point interaction. The effective Lagrangian for the spin-independent (scalar) interaction between a neutralino and a quark q is given by:

$$\mathcal{L}_{\text{eff}} = \sum_q a_q \bar{\chi}\chi\bar{q}q \,, \tag{4.36}$$

where a_q represents the effective coupling constant. The primary contribution to a_q arises from the exchange of the light (h^0) and heavy (H^0) Higgs bosons.

The neutralino-neutralino-Higgs couplings, denoted as $C_{\chi\chi h}$ and $C_{\chi\chi H}$, depend on the mixing of the lightest neutralino. The quark-quark-Higgs couplings are proportional to the quark masses and depend on the MSSM mixing angles α (the mixing angle of the CP-even Higgs sector) and β (where $\tan\beta = v_u/v_d$ is the ratio of the vacuum expectation values(vev)).

For up-type quarks (u, c, t), the couplings relative to the Standard Model Higgs coupling are:

$$g_{uuh} = \frac{\cos\alpha}{\sin\beta}\,, \quad g_{uuH} = \frac{\sin\alpha}{\sin\beta}\,. \tag{4.37}$$

For down-type quarks (d, s, b):

$$g_{ddh} = -\frac{\sin\alpha}{\cos\beta}\,, \quad g_{ddH} = \frac{\cos\alpha}{\cos\beta}\,. \tag{4.38}$$

Evaluating the Feynman diagrams for t-channel h^0 and H^0 exchange in the limit of zero momentum transfer, the effective coupling a_q is constructed by multiplying the vertices and the Higgs propagator $1/m_{H_i}^2$:

$$a_q = \frac{m_q}{v}\left(\frac{C_{\chi\chi h}g_{qqh}}{m_{h^0}^2} + \frac{C_{\chi\chi H}g_{qqH}}{m_{H^0}^2}\right)\,, \tag{4.39}$$

where $v \approx 246$ GeV is the electroweak vacuum expectation value.

B.2 WIMP-Nucleon Coupling

[17, 28, 37, 18] To find the effective WIMP-nucleon coupling f_N (where $N = p, n$ for proton and neutron), we must evaluate the nucleon matrix elements of the quark scalar currents:

$$f_N = \sum_{q=u,d,s,c,b,t} a_q \langle N|\bar{q}q|N\rangle \,. \tag{4.40}$$

For light quarks (u, d, s), the matrix elements are conventionally parameterized by the mass fractions $f_{Tq}^{(N)}$:

$$m_q \langle N|\bar{q}q|N\rangle = m_N f_{Tq}^{(N)} \,. \tag{4.41}$$

The heavy quarks (c, b, t) do not have a valence presence in the nucleon, but they interact with the nucleon via gluon exchange. Using the QCD trace anomaly, the heavy quark contribution can be related to the gluon field strength tensor, giving,

$$m_Q \langle N|\bar{Q}Q|N\rangle = \frac{2}{27} m_N f_{TG}^{(N)} \,, \quad \text{for } Q = c, b, t \,, \tag{4.42}$$

where $f_{TG}^{(N)} = 1 - \sum_{q=u,d,s} f_{Tq}^{(N)}$.

Substituting the matrix elements back into the equation for f_N, we factor out the quark mass dependence from a_q (letting $a_q \equiv \frac{m_q}{v} \tilde{a}_q$ where $\tilde{a}_q$ is the mass-independent coupling factor), Hence,

$$f_N = m_N \left[\sum_{q=u,d,s} \frac{a_q}{m_q} f_{Tq}^{(N)} + \frac{2}{27} f_{TG}^{(N)} \sum_{Q=c,b,t} \frac{a_Q}{m_Q} \right] . \tag{4.43}$$

B.3 Zero-Momentum-Transfer Cross Section

[31, 25] For a target nucleus $\mathcal{N}$ containing Z protons and $A - Z$ neutrons, the scalar interactions add coherently because the de Broglie wavelength of the non-relativistic WIMP is larger than the nuclear radius. The WIMP-nucleus coupling is the sum of the individual nucleon couplings:

$$f_{\mathcal{N}} = Z f_p + (A - Z) f_n \,. \tag{4.44}$$

The spin-independent scattering cross section evaluated at zero momentum transfer $(q \to 0)$ is then given by standard Fermi Golden Rule formulations:

$$\sigma_0 = \frac{4\mu_{\mathcal{N}}^2}{\pi} f_{\mathcal{N}}^2 = \frac{4\mu_{\mathcal{N}}^2}{\pi} \left[Z f_p + (A - Z) f_n \right]^2 \,, \tag{4.45}$$

where $\mu_{\mathcal{N}} = \frac{m_\chi m_{\mathcal{N}}}{m_\chi + m_{\mathcal{N}}}$ is the reduced mass of the WIMP-nucleus system. Since $f_p \approx f_n$ in most MSSM scenarios, the cross section scales roughly as A^2, which strongly motivates the use of heavy targets (like Xenon) in direct detection experiments.

B.4 Finite-Momentum Form Factor

[31, 25]

In realistic experimental collisions, the momentum transfer $q = \sqrt{2 m_{\mathcal{N}} E_R}$ (where E_R is the nuclear recoil energy) is finite. The assumption that the WIMP scatters coherently off the entire nucleus begins to break down as the momentum transfer increases, leading to a suppression of the cross section.

This spatial distribution of nucleons is accounted for by the nuclear form factor $F(q^2)$. The differential cross section with respect to the momentum transfer squared is written as:

$$\frac{d\sigma}{dq^2} = \frac{\sigma_0}{4\mu_{\mathcal{N}}^2 v_\chi^2} F^2(q^2) \,, \tag{4.46}$$

where v_χ is the WIMP velocity relative to the target.

The standard choice for spin-independent scattering is the Helm form factor, which treats the nucleus as a sphere with a softened edge:

$$F(q^2) = \frac{3 j_1(qR_1)}{qR_1} e^{-q^2 s^2/2} \,, \tag{4.47}$$

where $j_1(x) = (\sin x - x\cos x)/x^2$ is the spherical Bessel function of the first kind. The parameters are defined as follows:

- $s \approx 0.9$ fm characterizes the skin thickness of the nucleus.
- $R_1 = \sqrt{R^2 - 5s^2}$ is the effective nuclear radius.
- $R \approx 1.2A^{1/3}$ fm is the physical nuclear radius.

gives us our desired result.